

HIGH BALLISTIC COEFFICIENT MARS EDL WITH SUPERSONIC RETROPROPULSION

Connor Noyes*, Aron Wolf†, and Joel Benito‡

INTRODUCTION

Future Mars missions will require the ability to land increasingly heavy systems with high precision, possibly at high altitude landing sites. A key obstacle in landing systems with high ballistic coefficient is Mars' very thin atmosphere, approximately one hundred times less dense than Earth's atmosphere. As a result, hypersonic deceleration occurs slowly throughout atmospheric entry and additional deceleration methods are required before landing. Previous landers up to and including MSL relied on Viking-heritage technologies including a Disk-Gap-Band (DGB) supersonic parachute and a blunt body aeroshell.¹ Safe and effective deployment of a DGB parachute can be accomplished only within prescribed bounds on dynamic pressure and Mach number.² In addition to the restrictive constraint this imposes on the entry trajectory, there is a concern that for a parachute to effectively slow an entry vehicle with a high ballistic coefficient, its diameter must be large enough to impose certification costs, modeling uncertainty, or mission risk that could be unacceptable. This has prompted investigation into alternative mission concepts based on use of supersonic retropropulsion (SRP) without a parachute. This work investigates SRP as an enabling technology for Mars EDL of high ballistic coefficient vehicles.

PROBLEM FORMULATION

The primary objective is to examine the feasibility and scalability of Mars EDL for vehicles with high ballistic coefficients based on SRP technology. The EDL problem is divided into multiple phases and posed as the solution to a two point boundary value problem. The four phases are

1. Pre-entry: During this first phase the vehicle holds a constant bank angle with the lift vector oriented downward.
2. Entry: The vehicle is controlled via modulation of its bank angle toward the optimal ignition point.

*Engineering Graduate Student, EDL Guidance and Control Systems, Jet Propulsion Laboratory, California Institute of Technology, Pasadena, CA 91109 USA.

†Principal Guidance and Control Engineer, Guidance and Control Section, Jet Propulsion Laboratory, California Institute of Technology, Pasadena, CA 91109 USA.

‡Guidance and Control Engineer, EDL Guidance and Control Systems, Jet Propulsion Laboratory, California Institute of Technology, Pasadena, CA 91109 USA.

©Copyright 2017 California Institute of Technology. U.S. Government sponsorship acknowledged.

3. Pre-SRP: The vehicle is oriented to fly lift up and performs necessary operations such as altimetry measuring prior to ignition. This phase has a fixed 10 s duration.
4. SRP: The vehicle is delivered to the target altitude via retropropulsion and optimization is terminated.

The objective is to maximize the final landed mass in order to deliver the most payload to the surface. The following quantities are optimized

- Initial flight path angle at pre-entry
- Pre-entry duration
- Bank angle profile during atmospheric entry
- SRP ignition point
- SRP thrust magnitude and direction profiles

There are a number of constraints imposed. A minimum altitude constraint is applied in all phases to prevent subsurface flight. Minimum bank angle is set to 25° to preserve some control authority, and similarly the maximum bank angle allowed is 145° . The only terminal position constraint is on the landing altitude, no other restrictions are imposed (i.e. a fixed latitude and longitude is not targeted). All trajectories terminate at a final velocity of 1 m/s. No constraint is placed on the flight path angle during entry, so trajectories may loft if it is optimal to do so.

There are also a number of assumptions and models underlying the problem. MarsGRAM is used as a model of the Martian atmosphere. Aerodynamic coefficients are modeled as constant values. Aerodynamic forces acting on the vehicle are assumed to be zero once the engine has been ignited³ during the SRP phase. Even if this assumption does not hold in truth, it is common for unmodeled dynamics to be treated as disturbances in guidance algorithm development⁴ and so a similar approach may be adopted in this optimization-based study. Thrust is assumed to be applied with no cant angle, and without supersonic losses. SRP consists of only one phase with no attitude constraints at ignition. Real landing scenarios will have additional phases such as hover, constant velocity, or constant deceleration. A small adjustment in consideration of such possible phases are accounted for via a small addition to total propellant based on the cost of a 20s duration hover. Finally, the solution to the resulting optimal control problem is found via GPOPS-II.⁵

PARAMETRIC ANALYSIS

The estimation of sensitivities to design parameters is valuable to facilitate system and design trades. Tables 2 and 1 list the common vehicle characteristics, ballistic coefficients (BCs) and corresponding entry masses considered for parametric investigation. Additionally, the results of this section consider a simplified control parametrization in which the throttle is fixed at 90% and the thrust angle is optimized but held constant throughout the SRP braking.

Figure 1 shows that propellant mass fraction (PMF) is not affected by entry speed. For the ballistic coefficient of 450 kg/m^2 there is a roughly 1% increase in PMF for imposing a 4g constraint on the maximum g-load during entry. Trajectories that enter faster will naturally travel farther and will experience greater heat loading but Figure 2 shows that toward the end of the entry phase the

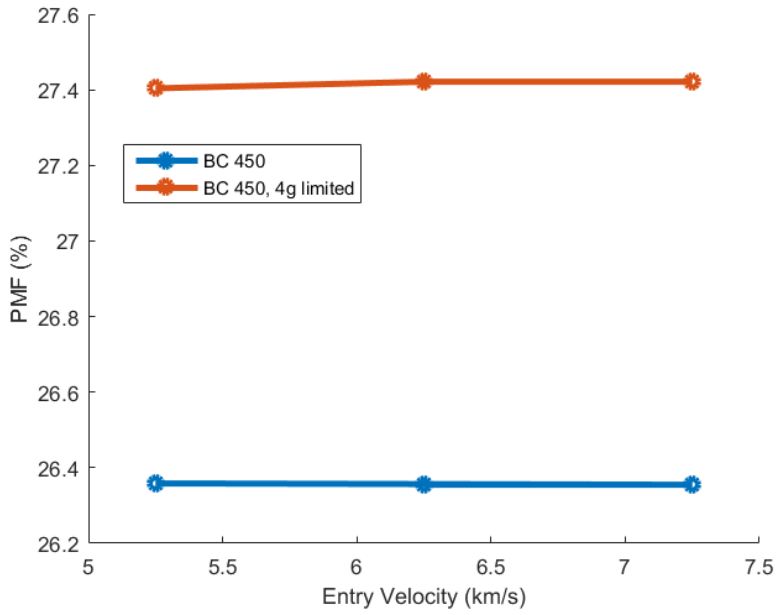


Figure 1. PMF is insensitive to entry speed.

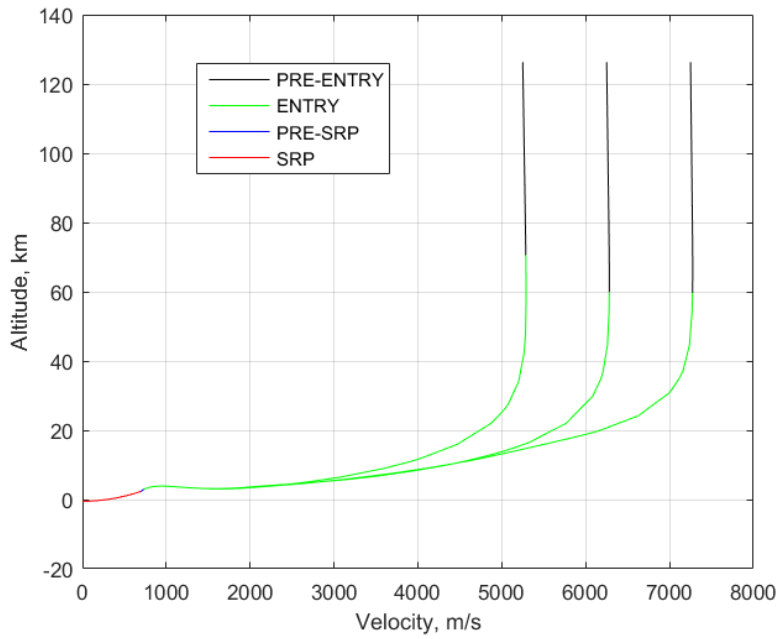


Figure 2. Trajectories with highly different entry speeds converge to the same SRP ignition conditions.

Ballistic Coefficient (kg/m ²)	Entry Mass (kg)
300	7625
450	11,440
600	15,250

Table 1. Ballistic coefficients and corresponding entry masses considered.

Parameter	Value
Aeroshell diameter (m)	4.7
Drag coefficient	1.47
Lift coefficient	0.353
Specific impulse (s)	295
Thrust-to-weight ratio	3
Inertial entry speed (km/s)	6.5

Table 2. Nominal parameters used in optimization.

trajectories converge in the altitude-velocity space prior to ignition, resulting in little to no difference in propellant consumption.

Figure 3 shows the sensitivity of PMF to the site altitude being targeted. The relationship is approximately linear because the resulting ignition velocities are also approximately linear in target altitude when entry flight path is also adjusted. The 4g constraint once again requires slightly more than 1% increase in PMF, while increasing the BC to 600 kg/m² (a 33% increase) shows about 3% increase in PMF. In general, g-limited cases have significantly shallower entry flight path angles which result in shallow trajectories with long downrange distances. The maximum g-load without a constraint imposed tends to be in the range 10-15g.

SRP CONTROLLABLE SET ANALYSIS

The controllable set for a given reference vehicle configuration is estimated numerically via optimization. The problem is constrained to longitudinal motion only. The controllable set is defined as the set of all initial conditions from which the target can be reached via SRP subject to limitation on the available fuel onboard the vehicle.

Estimation Procedure

Consider a simplified state vector $X^T = [x, y, u, v, m]$ where x is the current range to target, y is altitude above the target, u and v are the horizontal and vertical components of the planet-relative velocity, and m is the mass of the lander. A fixed (V_{SRP}, γ_{SRP}) pair is chosen to represent the conditions at ignition, i.e. at the beginning of SRP. The first step is to solve two problems to find the minimum and maximum distances to the target that can be flown by the vehicle by solving the following two optimal control problems:

$$\min J = x \tag{1}$$

$$\max J = x \tag{2}$$

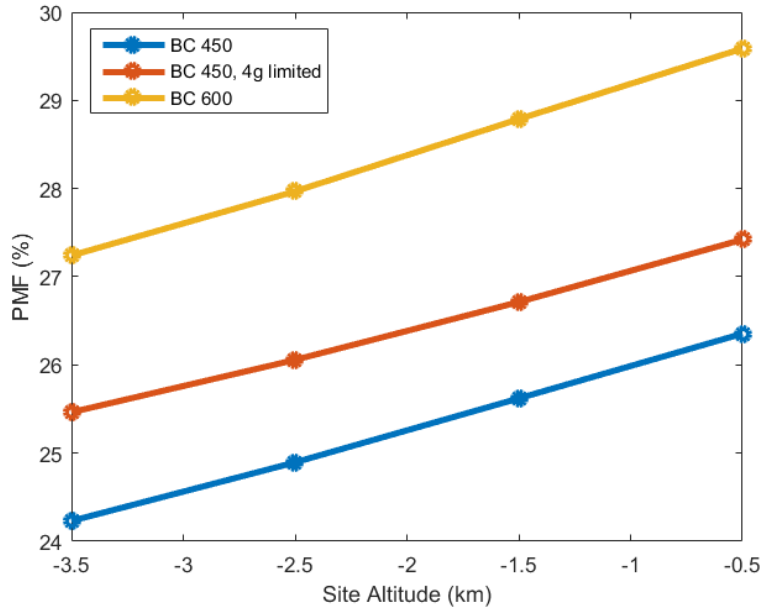


Figure 3. PMF is linear in target site altitude.

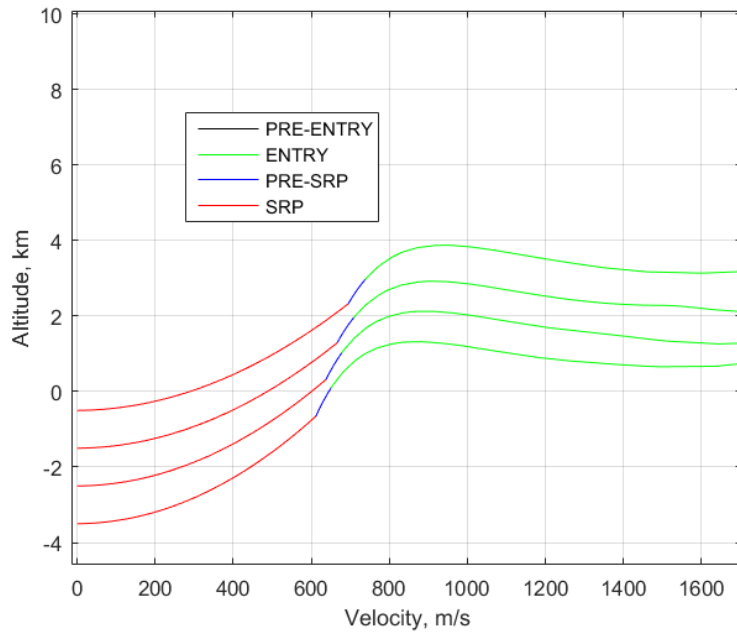


Figure 4. Trajectories targeting higher altitudes ignite at faster speeds resulting in higher propellant usage.

subject to the dynamics

$$\dot{x} = u \quad (3)$$

$$\dot{y} = v \quad (4)$$

$$\dot{u} = \frac{T}{m} \cos \mu \quad (5)$$

$$\dot{v} = \frac{T}{m} \sin \mu - g \quad (6)$$

$$\dot{m} = -\frac{T}{I_{sp}g_0} \quad (7)$$

and the boundary conditions

$$u(t_0) = -V_{SRP} \cos \gamma_{SRP} \quad (8)$$

$$v(t_0) = V_{SRP} \sin \gamma_{SRP} \quad (9)$$

$$m(t_0) = m_0 \quad (10)$$

$$x(t_f) = 0 \quad (11)$$

$$y(t_f) = 0 \quad (12)$$

$$u(t_f) = 0 \quad (13)$$

$$v(t_f) = 0 \quad (14)$$

$$m(t_f) \geq m_{dry} \quad (15)$$

where T is the thrust magnitude and μ is the thrust angle measured from the local forward horizontal. Additionally the vehicle's altitude is constrained to prevent subsurface flight.

The range $[x_{\min}, x_{\max}]$ is then discretized into n_x partitions. For each value x_i in the partition, the minimum and maximum altitude is determined via solution of $\min J = y$ and $\max J = y$ subject to the same dynamics, and the same boundary conditions with the additional condition that $x(t_0) = x_i$. The result is $2n_x$ points on the boundary of the controllable set for a fixed initial velocity. Finally, these steps are repeated for a range of (V_{SRP}, γ_{SRP}) pairs to cover the entire 4-D space. The method is easily generalizable to 3-D where the controllable set will be 6-D.

The size of the set alone is valuable information, but an additional step may be taken to determine the PMF value at points in the set's interior as well by solving $J = \max m(t_f)$ subject to fully fixed initial conditions.

Application

The above procedure is applied to estimate controllable sets for the reference vehicle under various conditions and assumptions. The SRP formulation ignores drag so the set will be invariant between different ballistic coefficients so long as the same thrust-to-weight ratio is maintained. The maximum PMF is set to 25% and it is assumed that the vehicle cannot throttle lower than 10% of maximum thrust. The range of velocities and flight path angles to use is based on experience from the parametric studies. The optimized results from the study indicate that the SRP phase for the vehicle in consideration typically begins at shallow flight path angles $-25^\circ \leq \gamma \leq 0^\circ$ and ignition velocities between 400-700 m/s.

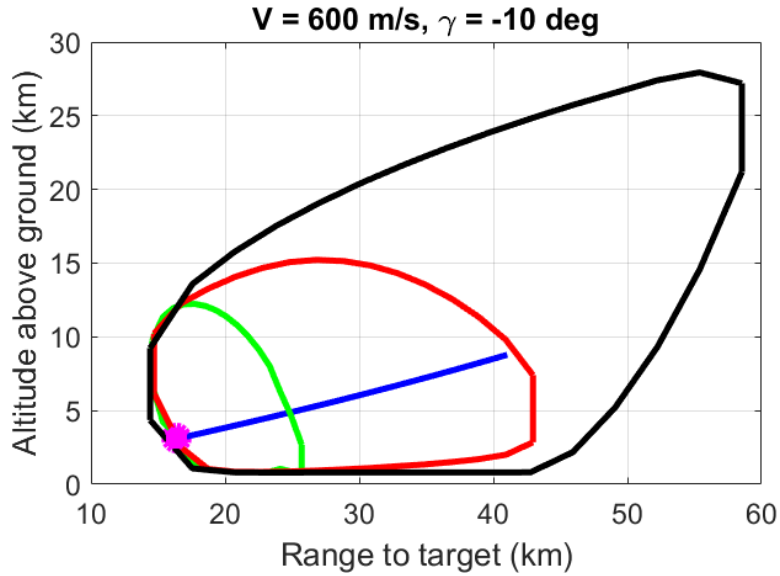


Figure 5. The outer black line gives the boundary for free (μ, T) , the red line for fixed T , the green line for T fixed at its maximum, and the blue line for fixed (μ, T) . The PMF optimal point is given by the magenta star.

Sensitivity A form of qualitative “sensitivity” of the controllable set is investigated by considering three different formulations of the powered descent phase. The simplest holds the thrust magnitude and direction to be constant values. The second allows the thrust direction to vary with time while thrust magnitude is held constant. A variation of this fixes the thrust magnitude at its maximum value. Lastly, both the thrust magnitude and its direction are permitted to vary along the trajectory. It is well known that thrust profiles for fuel-optimal powered descent trajectories for a point-mass are bang-bang and may have one, two, or three thrust arcs.^{6,7,10} Thus it is anticipated that each simpler formulation will produce a subset of the others.

Figure 5 shows the effect of each formulation on the size of controllable set at $(V, \gamma) = (600\text{m/s}, -10^\circ)$ for $\frac{T}{W} = 3$. It is not surprising that for the simplest parametrization the set is a line with no interior because the direction of thrust is given based on the required change in velocity and total time of flight. Thus for a fixed initial (u, v) only the thrust magnitude setting is available to meet both altitude and downrange targets, so the number of parameters is insufficient to meet all of the terminal constraints except when the target happens to be at the correct downrange at ignition. Put another way, for a given (V, γ, T) there is only one constant μ that will deliver the vehicle to the target altitude (if it is reachable at all) and thus there is only one corresponding range to go. Allowing the thrust direction to vary with time allows for some flexibility in altitude range, even when considering a fixed, maximal value for the throttle. The full optimized set is noticeably larger but much of the space is likely to be unused in nominal flight because optimal triggering is always lower and closer to the target. In off-nominal flight, such as the necessity of a large divert maneuver, however, the additional freedom may be useful.

The effect of varying thrust-to-weight on one slice of the controllable set is quantified in Figure 6. Naturally each doubling of this ratio allows the vehicle to approach the target altitude and position more closely before ignition is required. The control parametrization used in each case is a fixed throttle setting and free thrust direction and thus the black curve in Figure 6 is the same as the red

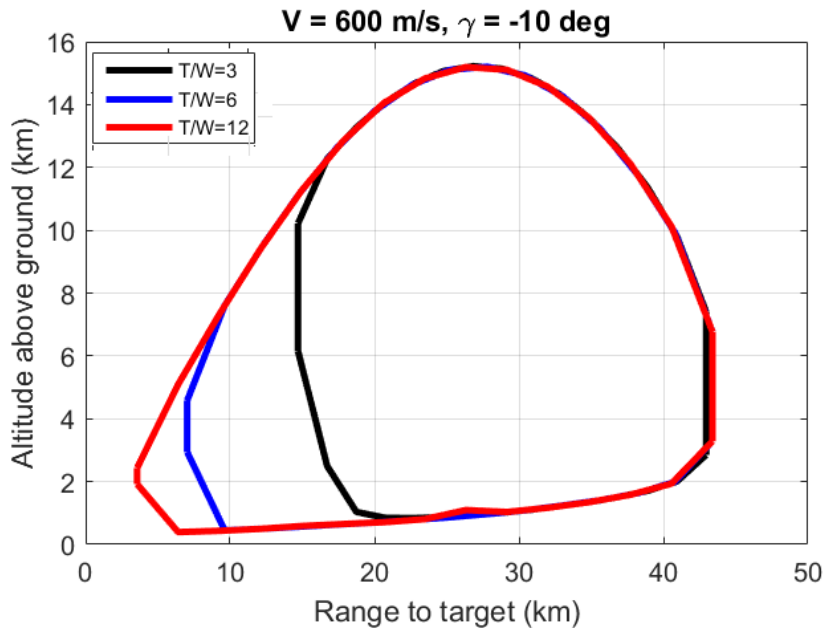


Figure 6. Three different thrust to weight ratios are compared for a fixed throttle and free μ parametrization.

curve of Fig 5.

Target Biasing The set is estimated for all combinations of $V \in [400, 500, 600]$ m/s and $\gamma \in [-2^\circ, -10^\circ, -20^\circ]$, and the PMF contours of the interior of each “slice” are approximated by 75 trajectories. The result is shown in Figure 7. Clearly, the optimum point at each ignition velocity and flight path is low and as close to the target as possible. However, there is also a gap in downrange distance where the vehicle is too close to the target and is incapable of arresting its velocity in time. A small portion of the set closest to the target will actually overshoot the target and turn back to reach it. This is a very expensive maneuver and so only very mild overshoots can be accommodated within the 25% PMF limit.

Notice that points significantly farther than the optimum can still reach the target, while as discussed there are some points closer than the optimum which are not in the set. This asymmetry implies that it is preferable to “stretch” trajectories out by igniting farther from the target than to wait until velocity is lower but the target is too close.

Consider an optimized trajectory that ignites at the fuel-optimal point and lands at some downrange from the entry point. With the same entry flight path angle, how would optimal trajectories look if they had to reach the same target in, e.g., $\pm 20\%$ atmospheric density? It turns out that while the denser case is not an issue, the thinner case experiences a large spike in required propellant because the vehicle cannot decelerate sufficiently upon reaching suitable ignition ranges. While the nominal and +20% cases ignite around 500 m/s, the -20% case ignites at a staggering 1100 m/s. The SRP phase of each trajectory is shown in altitude and range in Figure 8. Note that the high cost is due to high ignition speed, and not the larger range flown. By accepting some sub-optimality and biasing the target farther downrange, some cases will have to fly longer trajectories but the overall PMF cost will be more uniform. This is a trade between performance and robustness. Compare to Figure 9 in which the target is biased 10 km farther such that -20% density case can reach the

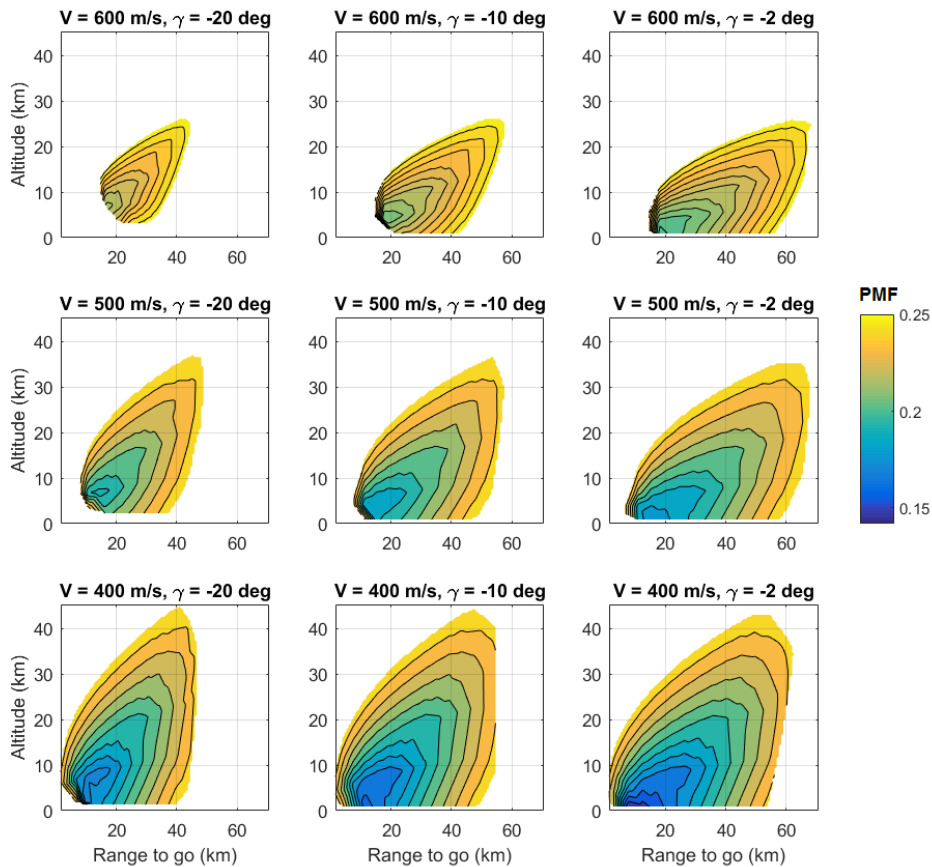


Figure 7. Several slices of the controllable set for a vehicle with thrust-to-weight of 3, colored by the PMF associated with landing from each ignition condition.

controllable set. Observe in table 3 that the ignition velocities are much more similar and thus there are no large changes in required propellant. Note that the control variables are still free in the dispersed atmosphere cases, with the understanding that any real guidance algorithm will perform suboptimally compared to the “non-deterministic” optimization bank angle profile, ignition point, and SRP maneuver.

CONCLUSION

An optimization based approach to feasibility and scalability of Mars EDL via supersonic retro-propulsion appears to have no high level impediments for even very high ballistic coefficients and low L/D type vehicles. Moving forward, higher fidelity modeling and simulation based results will be needed to refine the analysis. Removing the simplifying assumptions will increase the estimates of the propellant required but is unlikely to impact the broad trends shown herein. Analysis based on the controllable set of a given vehicle was presented, and used to make practical decisions concerning reference trajectories. A simulation based investigation should be pursued to confirm or deny the benefits of target biasing presented in the controllable set section, as well as to determine the effects of deterministic entry guidance and navigation system errors on SRP performance.

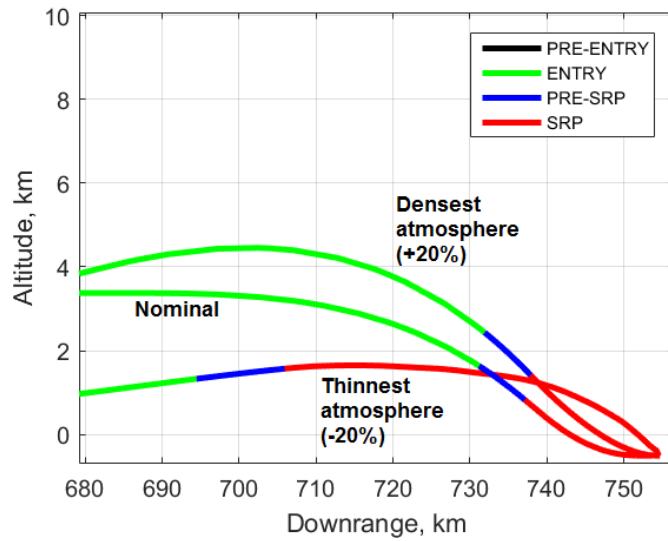


Figure 8. The case in less dense atmospheric ignites at a velocity twice that of the other two cases, incurring a very high propellant cost.

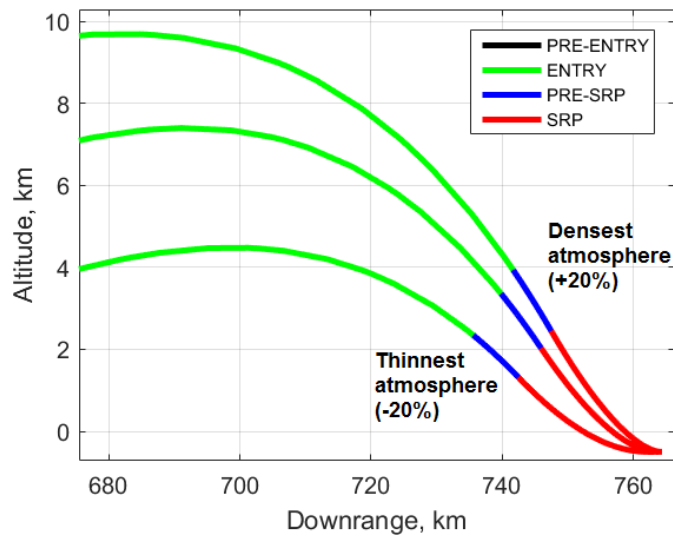


Figure 9. Biasing the target (in the nominal case) allows dispersed cases to remain feasible.

Case	Ignition Velocity (m/s)	PMF
Nominal Atmosphere	590	24%
+20% Density	582	24%
-20% Density	1100	36%
Target Biased Nominal	610	25%
Target Biased +20% Density	585	24%
Target Biased -20% Density	680	26%

Table 3. Ignition velocities and PMF with dispersed atmosphere, with and without target biasing.

ACKNOWLEDGMENTS

The research was carried out at the Jet Propulsion Laboratory, California Institute of Technology, under a contract with the National Aeronautics and Space Administration.

REFERENCES

- [1] Braun, R. D. and Manning, R. M., "Mars Exploration Entry, Descent and Landing Challenges," *Journal of Spacecraft and Rockets*, Vol. 44, No. 2, 2007, pp. 310-323.
- [2] Way, D. W., "On the Use of a Range Trigger for the Mars Science Laboratory Entry, Descent, and Landing," *IEEE*, 2011.
- [3] Korzun, A. M., Cruz, J. R., and Braun, R. D., "A Survey of Supersonic Retropropulsion Technology for Mars EDL," *IEEE*, 2007.
- [4] Rea, J. R., "An investigation of fuel optimal terminal descent," 2009.
- [5] Patterson, M., and Rao, A., "GPOPS-II: A MATLAB Software for Solving Multiple-Phase Optimal Control Problems Using hp-Adaptive Gaussian Quadrature Collocation Methods and Sparse Nonlinear Programming," *ACM Transactions on Mathematical Software*, Vol. 41, Issue 1, 2014.
- [6] Lawden, D. F., "Optimal Trajectories For Space Navigation," Butterworths, London, 1963.
- [7] Marec, J. P., "Optimal Space Trajectories," Elsevier, New York, 1979.
- [8] Samareh, J. A., Komar, D. R., "Parametric Mass Modeling for Mars Entry, Descent, and Landing System Analysis Study," *AIAA*, 2011.
- [9] Acikmese, B., and Ploen, S. R., "Convex Programming Approach to Powered Descent Guidance for Mars Landing," *Journal of Guidance, Control, and Dynamics*, Vol. 30, No. 5, 2007, pp. 1353-1366.
- [10] Topcu, U., Casoliva, J., and Mease, K. D., "Minimum-fuel powered descent for mars pinpoint landing," *Journal of Spacecraft and Rockets*, Vol. 44, No. 2, 2007.